



Short communication

Highly stabilized α -NiCo(OH)₂ nanomaterials for high performance device application

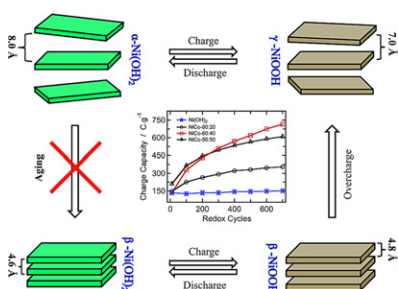
Paulo Roberto Martins, André Luis Araújo Parussulo, Sergio Hiroshi Toma, Michele Aparecida Rocha, Henrique Eisi Toma, Koiti Araki*

Instituto de Química, Universidade de São Paulo, Av. Prof. Lineu Prestes, 748, São Paulo, SP CEP 05508-000, Brazil

HIGHLIGHTS

- Fully nanostructured high charge capacity materials.
- Charge–discharge over 700 times without charge capacity loss.
- First stable α -nickel hydroxide nanomaterials.

GRAPHICAL ABSTRACT



ARTICLE INFO

Article history:

Received 14 May 2012

Received in revised form

15 June 2012

Accepted 18 June 2012

Available online 23 June 2012

Keywords:

Nickel hydroxide

Mixed hydroxides

Alpha-polymorph

Nanoparticles

Nanostructured materials

ABSTRACT

Improving the charge capacity, electrochemical reversibility and stability of anode materials are main challenges for the development of Ni-based rechargeable batteries and devices. The combination of cobalt, as additive, and electrode material nanostructuring revealed a very promising approach for this purpose. The new α -NiCo mixed hydroxide based electrodes exhibited high specific charge/discharge capacity (355–714 C g^{−1}) and outstanding structural stability, withstanding up to 700 redox cycles without any significant phase transformation, as confirmed by cyclic voltammetry, electrochemical quartz crystal microbalance and X-ray diffractometry. In short, the nanostructured α -NiCo mixed hydroxide materials possess superior electrochemical properties and stability, being strong candidates for application in high performance batteries and devices.

© 2012 Elsevier B.V. All rights reserved.

1. Introduction

Nickel hydroxides have been explored as electroactive materials of sensors [1–6], electrochromic devices [7] and rechargeable batteries [8,9]. Many efforts have been directed to improve the conductivity and reversibility of the charge/discharge processes, and to enhance the specific charge capacity by incorporation of

transition and non-transition metal ions as additives (Al, Zn, Cd, Co and Mn), [10–16] or by generating nanomaterials. Another possibility is by stabilizing and using the α -Ni(OH)₂ ($\alpha \leftrightarrow \gamma$, 433 mA h g^{−1}) instead of the conventional beta ($\beta \leftrightarrow \beta$, 289 mA h g^{−1}) polymorph, because of its superior electrochemical properties [17,18].

The addition of Co ions to Ni hydroxide electrodes is known to have beneficial effects, reducing the mechanical stress during charge/discharge processes, thus preventing electrode failure, and increasing the charge density [19,20]. However, the absence of the characteristic cobalt waves in the mixed NiCo hydroxides

* Corresponding author. Tel.: +55 11 3091 8513; fax: +55 11 3815 5640.

E-mail address: koiaraki@iq.usp.br (K. Araki).

voltammograms strengthened the hypothesis that only nickel is electrochemically active. Accordingly, the enhanced charge capacity [21] of mixed hydroxide materials was assigned to a higher conductivity and activation of more nickel sites rather than to contributions of cobalt sites [22]. For example, Kim et al. [23] showed that the α -phase material obtained by co-precipitation of 10.2% of cobalt(II) hydroxide with nickel(II) hydroxide was totally converted to the β -phase after 60 consecutive redox cycles, but the material containing 16.7% of cobalt was more stabilized. Similar results were described by Zhao et al. [24] by homogeneous co-precipitation of 16.8 and 19.5% of aluminium hydroxide by the urea method.

The specific charge capacity of β -Ni(OH)₂/Ni-foam electrodes is 275 mA h g⁻¹, lower than of β -Ni(OH)₂ nanotubes (315 mA h g⁻¹), but higher than that of nanosheets (219.5 mA h g⁻¹), commercial micrometer grade spherical powders (265 mA h g⁻¹) and microtubes (232.4 mA h g⁻¹) [28]. New routes for preparation of alpha nickel hydroxide nanomaterials, showing enhanced electrochemical properties and specific charge capacity, have also been reported [7,25–27] but none was stable enough for practical application.

Recently we showed that nanostructured materials prepared with α -Ni(OH)₂ nanoparticles can be stabilized [29,30], keeping the performance for at least 200 consecutive electrochemical cycles. In this report we demonstrate that the combination of the two strategies, more specifically, cobalt addition and nanostructuring, can further enhance the stability of alpha nickel hydroxide, resulting in more robust materials for application in batteries and other devices. In special, we disclose the electrochemical properties of nanostructured materials prepared from sol–gel nickel/cobalt mixed hydroxide nanoparticle precursors, exhibiting high specific charge capacity (up to 714 C g⁻¹) and stability in the α -phase (over 700 cycles).

2. Materials and methods

All reagents and solvents were of analytical grade and used as received. Isopropyl alcohol, *n*-butyl alcohol and potassium hydroxide were purchased from Synth. Anhydrous glycerin was purchased from Sigma–Aldrich, whereas nickel acetate tetrahydrate and cobalt acetate hydrate were obtained from Vetec.

The nickel/cobalt mixed hydroxide precursors were prepared by dissolving 4.82 mmol of the metal acetates in 25 mL of glycerin and adding 9.64 mmol of KOH in *n*-butanol, at room temperature. Four

samples were prepared and named according to the Ni:Co molar ratio as follows: Ni(OH)₂, NiCo-80:20, NiCo-60:40 and NiCo-50:50.

X-ray analyses were performed using a Higaku Miniflex powder diffractometer equipped with a Cu K α radiation source (1.541 Å, 30 kV, 15 mA, step = 0.02°), in the 2 θ range from 1.5 to 70°.

Cyclic voltammograms (–0.15–0.44 V, 20 mV s⁻¹) were registered on an Autolab PGSTAT30 potentiostat/galvanostat using a conventional three electrodes arrangement with a NiCo(OH)₂ modified fluorine doped tin oxide (FTO) as working electrode, a coiled platinum wire as auxiliary and an Ag/AgCl (in 1.0 mol dm⁻³ KCl, 0.222 V vs SHE) reference electrode, using 1.0 mol dm⁻³ KOH as electrolyte solution.

Electrochemical quartz crystal microbalance (EQCMB) measurements were carried out simultaneously with CV, using AT-cut quartz crystal electrodes (5 MHz, 25.4 mm diameter, working area = 1.37 cm²) covered with a thin platinum layer, and a Maxtek PM-710 equipment coupled with the Autolab PGSTAT30 potentiostat/galvanostat, using a conventional three electrodes arrangement.

FTO glass plates were carefully washed with isopropanol and water, dried in air and modified by spin-coating the nickel/cobalt mixed hydroxide sol–gel nanoparticle precursors, at 2500 rpm. These electrodes were dried under vacuum and calcined at 240 °C for 30 min. The specific charge capacities per gram of nickel were determined using 1.0 cm² electrodes, where the amounts of nickel and cobalt were measured by ICP-AES (Arcos-SOP – Spectro) using the solutions obtained by dissolving the NiCo hydroxide films with a 0.1 mol dm⁻³ nitric acid solution, from the working electrodes after 700 cycles. The quartz crystal electrodes were modified in a similar way, except for the exclusion of the heat treatment.

3. Results and discussion

Mixed alpha-NiCo(OH)₂ sol–gel precursors (α -NiCo-80:20, α -NiCo-60:40 and α -NiCo-50:50) are convenient raw materials for the preparation of nanostructured films by methods as simple as dip-coating and spin-coating. In fact, porous films constituted by agglomerated 5–15 nm nanoparticles, resembling sponge like nanostructures, were obtained in all cases. A typical SEM image of a NiCo-50:50 sample is shown in Fig. 1A where the particle size and morphology are clearly depicted. The vacuum dried material was stable enough to be washed and submitted to electrochemical cycling without significant lixiviation or flaking, but the calcined materials are more stable and used throughout, except for the

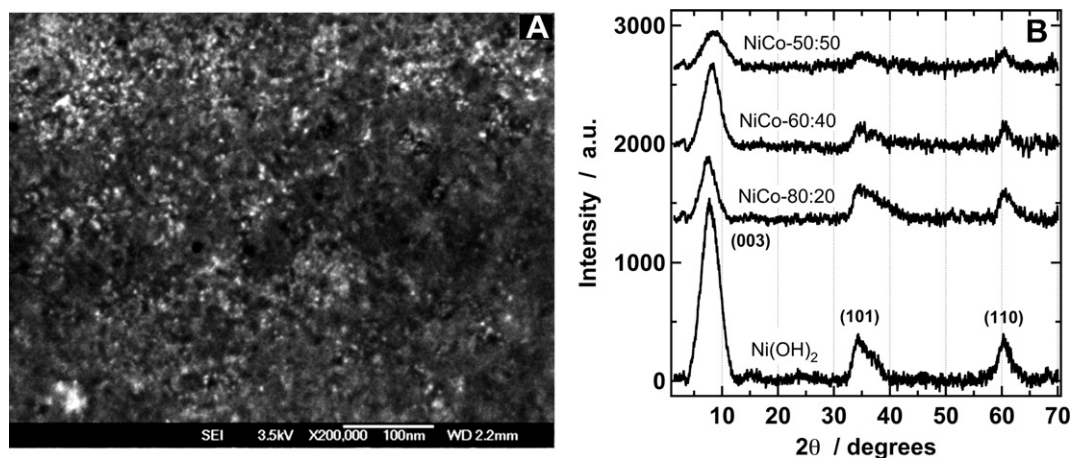


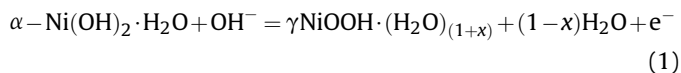
Fig. 1. (A) SEM image of a NiCo-50:50 electrode calcined at 240 °C, and (B) XRD of the nanostructured nickel and cobalt mixed hydroxide materials.

samples for EQCMB measurements which were not submitted to heat treatment to avoid damaging the quartz crystal.

The polymorphic phases of nickel hydroxide materials can be readily distinguished by X-ray diffractometry (XRD) by evaluating the inter-slab distances and the degree of organization of the lamella along the crystallographic *c* axis. The disordered turbostratic structure of α -Ni(OH)₂ presents inter-slab distances higher than about 8 Å, whereas the structure of the beta polymorph is more compact and organized presenting a much shorter inter-slab distance of 4.6 Å.

X-ray diffractograms of Ni(OH)₂, NiCo-80:20, NiCo-60:40 and NiCo-50:50 nanostructured materials are shown in Fig. 1B. Only the 003 peak was observed in the low angle region at 7.91°, 7.55°, 8.16° and 8.64°, respectively corresponding to inter-slab distances of 11.2, 11.7, 10.9 and 10.3 Å, in addition to lower intensity and broadened 101 (34.5°) and 110 (60.3°) peaks, confirming that the nanostructured materials are constituted by rather small sized crystallites of the α -polymorph. A tendency of decrease of inter-slab distances was observed as a function of cobalt content, but no significant shift of the 101 and 110 peaks could be observed precluding the comparison of lattice parameters. However, the substitution of Ni(II) by cobalt ions in the lattice should have contrasting effects depending on its oxidation state and extent of substitution since Ni(II) ionic radii (83 pm) is in between that of Co(II) and Co(III) (88.5 and 68.5 pm, respectively).

The electrochemical quartz crystal microbalance (EQCMB) experiments were carried out to shed light on possible structural changes that may be occurring along the successive charge/discharge processes. This technique is quite sensitive and convenient to distinguish the alpha and beta polymorphic phases. The α -Ni^{II}(OH)₂ is characterized by a positive mass change whereas the β -Ni^{II}(OH)₂ shows exactly the opposite behavior associated with the oxidation process but the mechanism is not clearly defined. Eq. (1) can be used to explain that behavior, but the incorporation of hydrated cations and hydroxide anion concomitantly with the release of water molecules during the oxidation process have also been proposed [23].



A typical EQCMB experiment for the NiCo nanomaterials is illustrated in Fig. 2 where the results for the NiCo-50:50 and the simultaneously measured CVs are depicted. The oxidation at $E_{\text{ap}} = +0.28$ V (Fig. 2A) is associated with a positive mass change that parallels the current rise in the respective voltammogram, indicating that both are correlated and the corresponding cathodic wave at $E_{\text{cp}} = +0.23$ V is associated with a negative mass change, as expected for nickel hydroxide nanomaterials in the alpha polymorphic phase. Surprisingly, the charge capacity and the EQCMB profile after 50 and 200 cycles were very similar clearly reflecting the electrochemical stability of the nanomaterial (Fig. 2B).

FTO electrodes modified with the nanomaterials were prepared by defining 1.0 cm² areas using Scotch tape, depositing the mixed NiCo hydroxide sol-gel nanoparticle precursors, drying under vacuum and firing at 240 °C. The CVs (Fig. 3) are characterized by low intensity redox waves that become well defined in the 0.2–0.4 V range after about ten redox cycles for electrode conditioning. The peak currents associated with the Ni^{II}(OH)₂/Ni^{III}OOH redox pair increased dramatically while small shifts on the anodic and cathodic peak potentials were observed, indicating an increase of the electroactive sites concentration as a function of the number of successive scans.

The voltammetric behavior of the thermally treated mixed hydroxides was strongly dependent on the amount of cobalt ion

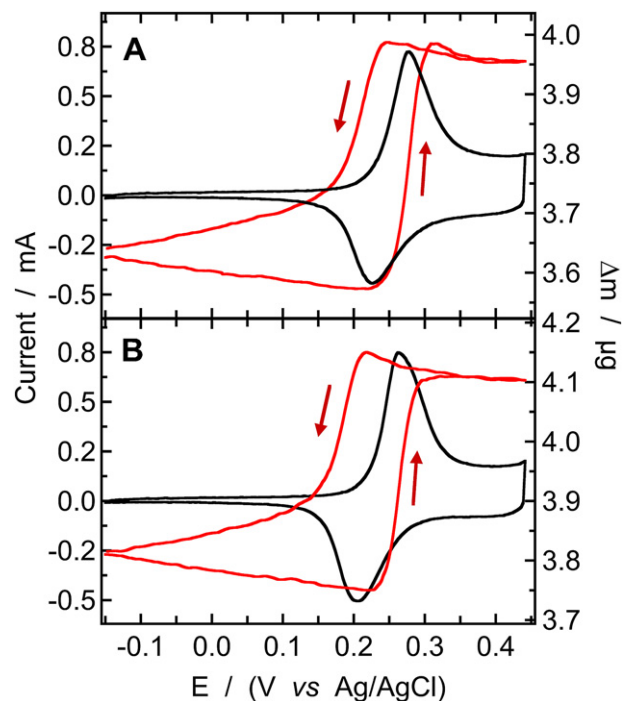


Fig. 2. Cyclic voltammogram (black line) and voltamassogram (red line) of α -NiCo-50:50 after (A) 50 and (B) 200 scan cycles, in 1 mol dm⁻³ KOH electrolyte solution, at 20 mV s⁻¹. (For interpretation of the references to color in this figure legend, the reader is referred to the web version of this article.)

present in the nanomaterials (Fig. 3A–D). For example, the E_{ap} and E_{cp} of pure Ni(OH)₂ were found respectively at +0.39 and +0.30 V. However, they were significantly shifted to lower potentials as the amount of cobalt was increased, such that E_{ap} was cathodically shifted to 0.37, 0.31 and 0.29 V respectively after incorporation of 20, 40 and 50% of cobalt to the Ni(OH)₂, improving the reversibility and decreasing the possibility of oxygen gas evolution during the charging process. Two successive CVs were always superimposable, except for a small increase in current, indicating that all electrochemically active sites were recovered during the reduction

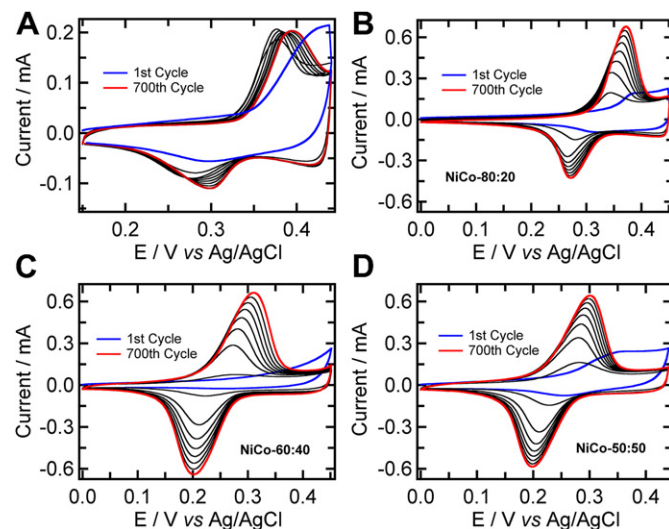


Fig. 3. Successive cyclic voltammograms of FTO electrodes modified with A) Ni(OH)₂, B) α -NiCo-80:20, C) α -NiCo-60:40 and D) α -NiCo-50:50 and submitted to heat treatment at 240 °C for 30 min, in 1 mol dm⁻³ KOH and scan rate = 20 mV s⁻¹.

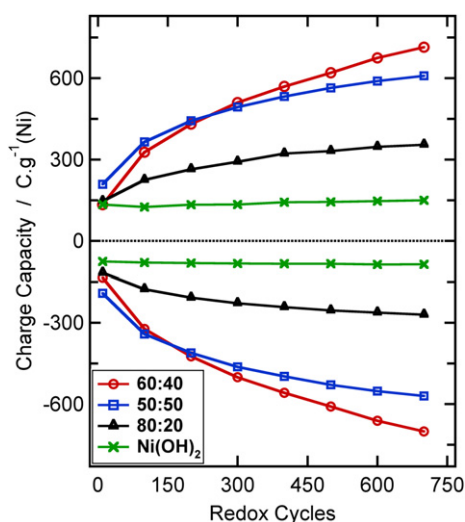


Fig. 4. Plots of the specific charge and discharge capacities per gram of nickel of FTO electrodes modified with stabilized pure and mixed alpha nickel hydroxides (α -Ni(OH)₂, α -NiCo-80:20, α -NiCo-60:40 and α -NiCo-50:50), fired at 240 °C for 30 min, as a function of the number of consecutive scan cycles in 1 mol dm⁻³ KOH, at 20 mV s⁻¹.

(discharge) process despite the slower kinetics, as indicated by the less intense and broader cathodic wave. The charge/discharge curves become more symmetric as the cobalt content was increased (Figs. 3 and 4).

The Ni:Co molar ratios in the modified electrodes were determined before (77.7:22.3, 56.4:43.6 and 47.3:52.7) and after 700 redox cycles (79.0:21.0, 58.1:41.9 and 53.3:46.7), and the specific charge and discharge capacities per gram of nickel were evaluated from the amounts of charge under the voltammetric waves (estimated by integration of CVs in Fig. 3) and the respective mass of nickel in the electrode determined by ICP-AES. It should be noticed that the charge capacity of the pure Ni(OH)₂ remained more or less constant (147 C g⁻¹(Ni)) whereas those of mixed hydroxides increased progressively as a function of the number of successive charge/discharge cycles, reaching limit values as high as 355, 714, and 609 C g⁻¹(Ni), respectively for the NiCo-80:20, NiCo-60:40 and NiCo-50:50 nanomaterials, after 700 cycles. The exception seems to be the NiCo-60:40, which should reach a limit value as high as five times the charge capacity of α -Ni(OH)₂. This behavior suggests that the diffusion of electrolyte and consequent activation of nickel hydroxide sites is somewhat slower in this material.

Considering nickel hydroxide as electrochemically active species, the coulombic efficiencies were estimated as 8.9, 21.6, 43.4 and 37.0%, respectively for α -Ni(OH)₂, α -NiCo-80:20, α -NiCo-60:40 and α -NiCo-50:50, indicating that almost half of the nickel hydroxide sites are electrochemically active. These results are inconsistent with a significant increase of the degree of crystallinity and conversion of the material to the β -phase polymorph, confirming the electrochemical stability and reversibility of the mixed hydroxide nanomaterials, in striking contrast with previously reported analogous materials.

4. Conclusion

Mixed nickel and cobalt hydroxide nanomaterials exhibiting enhanced electrochemical reversibility and specific charge and discharge capacity as a function of cobalt molar proportion up to

50% were successfully prepared from sol–gel precursors. Interestingly, the specific charge capacity increased progressively until up to 700 cycles and no change in the EQCM profile was observed confirming their high structural stability in the alpha polymorphic phase. The α -NiCo-60:40 showed the best performance exhibiting at least four and six times higher specific charge capacity than pure α -Ni^{II}(OH)₂ and β -Ni^{II}(OH)₂, respectively. Summarizing, the mixed hydroxide nanomaterials showed superior electrochemical properties and phase stability making them suitable for high charge device applications.

Acknowledgements

To Fundação de Amparo à Pesquisa do Estado de São Paulo (FAPESP) and Conselho Nacional de Desenvolvimento Científico e Tecnológico (CNPq) for the financial support.

Appendix A. Supplementary material

Supplementary material associated with this article can be found, in the online version, at <http://dx.doi.org/10.1016/j.jpowsour.2012.06.065>.

References

- [1] A. Salimi, E. Sharifi, A. Noorbakhsh, S. Soltanian, *Electrochem. Commun.* 8 (2006) 1499.
- [2] M. Jafarian, M.G. Mahjani, M.G. Heli, F. Gobal, M. Heydarpoor, *Electrochem. Commun.* 5 (2003) 184.
- [3] P.R. Martins, M.A. Rocha, L. Angnes, H.E. Toma, K. Araki, *Electroanalysis* 23 (2011) 2541.
- [4] J.Y. Park, K.S. Ahn, Y.C. Nah, H.S. Shim, Y.E. Sung, *J. Sol–Gel Sci. Technol.* 31 (2004) 323.
- [5] M. Vidotti, C.D. Cerri, R.F. Carvalhal, J.C. Dias, R.K. Mendes, S.I.C. de Torresi, L.T. Kubota, *J. Electroanal. Chem.* 636 (2009) 18.
- [6] M.S.M. Quintino, H. Winnischofer, K. Araki, H.E. Toma, L. Angnes, *Analyst* 130 (2005) 221.
- [7] J.Y. Qi, P. Xu, Z.S. Lv, X.R. Liu, A.H. Wen, *J. Alloy Compd.* 462 (2008) 164.
- [8] W. Zhang, W. Jiang, L. Yu, Z. Fu, W. Xia, M. Yang, *Int. J. Hydrogen Energy* 34 (2009) 473.
- [9] A.K. Shukla, S. Venugopalan, B. Hariprakash, *J. Power Sources* 100 (2001) 125.
- [10] K. Provazi, M.J. Giz, L.H. Dall'Antonia, S.I.C. de Torresi, *J. Power Sources* 102 (2001) 224.
- [11] K. Watanabe, M. Koseki, N. Kumagai, *J. Power Sources* 58 (1996) 23.
- [12] T.N. Ramesh, R.V. Kamath, *Electrochim. Acta* 53 (2008) 8324.
- [13] Y.W. Li, J.H. Yao, C.J. Liu, W.M. Zhao, W.X. Deng, S.K. Zhong, *Int. J. Hydrogen Energy* 35 (2010) 2539.
- [14] S.A. Cheng, A.B. Yan, H. Liu, J.Q. Zhang, C.N. Cao, *J. Power Sources* 76 (1998) 215.
- [15] M.Y. Wu, J.M. Wang, J.Q. Zhang, C.N. Cao, *J. Solid State Electr.* 10 (2006) 411.
- [16] W.H. Zhu, J.J. Ke, H.M. Yu, D.J. Zhang, *J. Power Sources* 56 (1995) 75.
- [17] R. Barnard, C.F. Randell, F.L. Tye, *J. Appl. Electrochem.* 10 (1980) 109.
- [18] P.V. Kamath, M. Dixit, L. Indira, A.K. Shukla, V.G. Kumar, N. Munichandraiah, *J. Electrochem. Soc.* 141 (1994) 2956.
- [19] H.H. Law, J. Sapjeta, *J. Electrochem. Soc.* 136 (1989) 1603.
- [20] R. Sjövall, *J. Power Sources* 90 (2000) 153.
- [21] M. Oshitani, H. Yufu, K. Takashima, S. Tsuji, Y. Matsumaru, *J. Electrochem. Soc.* 136 (1989) 1590.
- [22] I. Serebrennikova, V.I. Birss, *J. Electrochem. Soc.* 147 (2000) 3614.
- [23] M.S. Kim, K.B. Kim, *J. Electrochem. Soc.* 145 (1998) 507.
- [24] Y.L. Zhao, J.M. Wang, H. Chen, T. Pan, J.Q. Zhang, C.N. Cao, *Int. J. Hydrogen Energy* 29 (2004) 889.
- [25] F.F. Tao, M.Y. Guan, Y.M. Zhou, L. Zhang, Z. Xu, J. Chen, *Cryst. Growth Des.* 8 (2008) 2157.
- [26] G.T. Zhou, Q.Z. Yao, X.C. Wang, J.C. Yu, *Mater. Chem. Phys.* 98 (2006) 267.
- [27] X.Y. Guan, J.C. Deng, *Mater. Lett.* 61 (2007) 621.
- [28] Y. Wang, D.X. Cao, G.L. Wang, S.S. Wang, J.Y. Wen, J.L. Yin, *Electrochim. Acta* 56 (2011) 8285.
- [29] M.A. Rocha, H. Winnischofer, K. Araki, F.J. Anaissi, H.E. Toma, *J. Nanosci. Nanotechnol.* 11 (2011) 3985.
- [30] M.A. Rocha, F.J. Anaissi, H.E. Toma, K. Araki, H. Winnischofer, *Mater. Res. Bull.* 44 (2009) 970.